Spectrum-Free Estimation of Doppler Velocities Using Ultra-Wideband Radar

Sakamoto, Takuya; Akiyama, Daichi; Sato, Takuro; Sato, Toru

Received August 8, 2016, accepted September 16, 2016, date of publication October 3, 2016, date of current version March 28, 2017.

Digital Object Identifier 10.1109/ACCESS.2016.2614824

Spectrum-Free Estimation of Doppler Velocities Using Ultra-Wideband Radar

TAKUYA SAKAMOTO[1,2], (Member, IEEE), DAICHI AKIYAMA[2], TAKURO SATO[2], AND TORU SATO[2], (Member, IEEE)

[1]Graduate School of Engineering, University of Hyogo, Himeji 671-2280, Japan
[2]Graduate School of Informatics, Kyoto University, Kyoto 606-8501, Japan

Corresponding author: T. Sakamoto (t-sakamo@i.kyoto-u.ac.jp)

This work was supported in part by the Kyoto University SPIRITS Project, in part by the University of Hyogo Grant for Young Researchers, in part by the MEXT Center of Innovation Program, JSPS KAKENHI under Grant 25249057, Grant 15KK0243, and Grant 15K18077, and in part by the Research and Development Project for Expansion of Radio Spectrum Resources for More Efficient Use of Frequency Resources for the Future of the Ministry of Internal Affairs and Communications, Japan.

ABSTRACT A method for estimating Doppler velocities using ultra-wideband radar data is presented. Unlike conventional time–frequency analysis, the proposed method can directly obtain Doppler velocities without searching for peaks in a spectrum. By exploiting closed-form solutions for the Doppler velocities, it avoids the trade-off between time and frequency resolution, thus maintaining high time resolution. Both simulations and measurements are used to evaluate the proposed method versus conventional techniques.

INDEX TERMS Doppler measurement, signal resolution, ultra–wideband radar.

I. INTRODUCTION

Doppler velocity is one of the most important target parameters that radar systems are designed to measure. As reviewed in [1], the development of pulsed Doppler radar began in the 1940s [2]. Conventionally, target velocities have been measured from the variation of pulse-to-pulse phase rotation over time by applying a Fourier transform to the signals in the slow-time direction. Time–frequency analysis techniques have been developed to measure the time variation of frequencies, such as the short-time Fourier transform and Wigner distribution [3], [4]. These classical techniques suffer from a trade-off: higher time resolutions imply lower frequency resolutions. To overcome this limitation, elaborate methods have been studied, including the Choi–Williams distribution [5], the reassigned joint time–frequency transform [6], parametric spectrum estimation using the Capon method [7], and iterative adaptive Doppler spectrogram analysis [8].

In addition, micro-Doppler measurements are also of great interest in radar applications designed to monitor human targets [9]–[11]. This information allows one to form radar images using only a few fixed antennas [12]–[14] and to infer different types of activity from the spectral features [15]. With ultra-wideband radar systems, the Doppler spectrum can be calculated for each time and range, resulting in a three-dimensional range-Doppler surface [16]. This technique has proved particularly useful for monitoring human gait through micro-Doppler features. Such examples illustrate that although the estimation of Doppler velocities from radar signals has a long history, the topic is far from obsolete.

This paper proposes a new method for estimating a range-time image of a Doppler distribution using only local information, the derivatives of the radar signals, without forming spectra. This expands upon the conventional texture method, which can estimate only a single target velocity [17]. The proposed extended texture method is able to handle overlapping echoes and to estimate two Doppler velocities by exploiting closed-form solutions of a set of derivative equations. Unlike many time–frequency analysis tools, the proposed method does not use time windows, and thus the classical trade-off between time and frequency resolution does not apply, which allows it to achieve high time resolution. Conventional time–frequency analysis requires finding peaks in a spectrum to estimate targets' Doppler velocities, whereas the proposed method can obtain velocity solutions directly without searching. The proposed method produces an image that includes three important parameters, time, range, and Doppler velocity, which helps to analyze micro-Doppler signatures [16] to type-classify targets (e.g. humans, horses, and dogs) and actions (e.g. walking, running and crawling) in various security and safety applications such as through-wall detection and ground surveillance [18]–[20].

The system and signal models are introduced in Section II. Two conventional methods, the short-time Fourier transform and the texture method, are explained in Section III, which is followed by the derivation of the extended texture method, which can be applied to two overlapping echoes, in Section IV. In Section V, the conventional and proposed methods are applied to simulated data to evaluate their accuracy. In Section VI, the methods are applied to actual radar data measured from walking persons, and we demonstrate the performance of the proposed method in a realistic scenario. Discussions are presented in Section VII, and Section VIII concludes.

II. SYSTEM MODEL

We assume a quasi-monostatic radar system whose transmitting and receiving antennas, at positions $\boldsymbol{x}_T$ and $\boldsymbol{x}_R$, are located close together, i.e., $\boldsymbol{x}_T \simeq \boldsymbol{x}_R$. The signal $\rho(\tau)$ is transmitted from the antenna at $\boldsymbol{x}_T$, where τ is the fast-time. We assume multiple moving targets, of which the i-th target is located at $\boldsymbol{x}_i(t)$, where t is the slow time. The propagation path l_i for the i-th target is

$$\begin{aligned} l_i(t) &= |\boldsymbol{x}_i(t) - \boldsymbol{x}_T| + |\boldsymbol{x}_i(t) - \boldsymbol{x}_R| \\ &\simeq 2|\boldsymbol{x}_i(t) - \boldsymbol{x}_A|, \end{aligned} \tag{1}$$

where $\boldsymbol{x}_T \simeq \boldsymbol{x}_A$ and $\boldsymbol{x}_R \simeq \boldsymbol{x}_A$ are assumed for simplicity, where $\boldsymbol{x}_A = (\boldsymbol{x}_T + \boldsymbol{x}_R)/2$. In this case, the Doppler velocity $v_i(t)$ in the direction of the antennas for the i-th target is

$$v_i(t) = -\frac{d}{dt} l_i(t)/2. \tag{2}$$

A conventional B-scan radar signal is a function $\hat{s}(t, \tau)$ of two variables, the slow time t and fast time τ. Here, however, we use the range $r = c\tau/2$ as a variable instead of τ to simplify the mathematical expressions. As a result, the signal is expressed as $s(t, r) = \hat{s}(t, 2r/c)$, where c is the speed of light. Because the delay time for the i-th target is $\tau_i(t) = l_i(t)/c$, its corresponding range is

$$r_i(t) = c\tau_i(t)/2 = l_i(t)/2, \tag{3}$$

and thus

$$v_i(t) = \frac{d}{dt} r_i(t) \tag{4}$$

is the Doppler velocity for the i-th target.

Assuming two targets, let $p_1(r)$ and $p_2(r)$ respectively be the echo waveforms scattered from each. We assume that these waveforms are the output of a receiver's filter. The waveform $p_i(r)$ is not necessarily the same as the transmitted one because of waveform distortion due to scattering. We assume that $p_i(r)$ is independent of the range r_i for simplicity.

Thus, if there is only a single target, we model the received signal as

$$s_1(t, r) = p_1(t, r - r_1(t)). \tag{5}$$

If there are two targets in the scene, the signal is modeled as

$$s_2(t, r) = p_1(t, r - r_1(t)) + p_2(t, r - r_2(t)). \tag{6}$$

III. CONVENTIONAL METHODS FOR ESTIMATING DOPPLER VELOCITY

A conventional time–frequency analysis can separate echoes from different targets with different Doppler frequencies and also estimate the target velocity. One such method is the short-time Fourier transform, which applies Fourier transform to the time-windowed signal as

$$S(t, r, v) = \int s(t', r) w(t' - t) \exp\left(-jk_0 v t'\right) dt', \tag{7}$$

where $k_0 = 2\pi f_0/c$ is the wave number, f_0 is the center frequency, and w is the window function. The Doppler velocity v_D is then calculated as

$$v_D(t, r) = \arg\max_v |S(t, r, v)|^2. \tag{8}$$

The time resolution Δt is limited by the width $\Delta t = T_{obs}$ of the window $w(t)$, which also determines the frequency resolution $\Delta f = 1/T_{obs}$. To overcome this limitation, various elaborate time–frequency analysis techniques have been proposed, as mentioned above [3]–[8]. Nonetheless, time resolution must be sacrificed to improve frequency resolution in many of these methods.

Another approach to estimating Doppler velocities, called the texture method, was proposed in [17]. This method can only be applied to the single-target case, but is unique in that it uses only local derivatives of the received signal, without time windows. The target velocity can therefore be obtained directly without generating a Doppler spectrum. The texture method partially differentiates $s_1(t, r)$ in terms of t and r to obtain

$$\begin{aligned} \partial s_1(t, r)/\partial t &= v_1(t)\dot{p}_1(r - r_1(t)), \\ \partial s_1(t, r)/\partial r &= \dot{p}_1(r - r_1(t)), \end{aligned} \tag{9}$$

where $\dot{p}_1(r) = dp_1(r)/dr$ and Eq. (2) was used. By dividing $\partial s_1(t, r)/\partial t$ by $\partial s_1(t, r)/\partial r$, the target speed is obtained as

$$v_1(t) = \frac{\partial s_1(t, r)/\partial t}{\partial s_1(t, r)/\partial r}, \tag{10}$$

unless $\partial s_1(t, r)/\partial r = 0$.

Again, though, the texture method only applies when there is a single target in the scene. If there are two, the right-hand side of Eq. (10) becomes

$$\frac{\partial s_2(t, r)/\partial t}{\partial s_2(t, r)/\partial r} = \frac{v_1(t)\dot{p}_1(r - r_1(t)) + v_2(t)\dot{p}_2(r - r_2(t))}{\dot{p}_1(r - r_1(t)) + \dot{p}_2(r - r_2(t))}, \tag{11}$$

which is neither $v_1(t)$ nor $v_2(t)$. This shows why the texture method can only be used for a single target in the same range bin at the same time. It should be noted that the texture method does not use Fourier transforms, and thus the time resolution is preserved.

IV. EXTENDED TEXTURE METHOD FOR ESTIMATING DOPPLER VELOCITIES FROM OVERLAPPING ECHOES

We next derive our extension of the texture method to allow estimating two Doppler velocities from overlapping target

echoes. We assume the signal $s_2(t, r)$, which contains echoes from two targets, as in Eq. (6). For simplicity, we drop the subscript 2 in this section. Second-order partial derivatives of $s(t, r)$ are obtained as

$$\begin{aligned} s_{rr}(t, r) &= \ddot{p}_1(r - r_1) + \ddot{p}_2(r - r_2), \\ s_{tr}(t, r) &= v_1\ddot{p}_1(r - r_1) + v_2\ddot{p}_2(r - r_2), \\ s_{tt}(t, r) &= v_1^2\ddot{p}_1(r - r_1) + v_2^2\ddot{p}_2(r - r_2), \end{aligned} \tag{12}$$

$$\tag{13}$$

where $\ddot{p}_1(r) = d^2p_1(r)/dr^2$ and $\ddot{p}_2(r) = d^2p_2(r)/dr^2$. We also assume $s_{rr} = \partial^2 s/\partial r^2$, $s_{tr} = \partial^2 s/\partial t\,\partial r$, and $s_{tt} = \partial^2 s/\partial t^2$. There are four unknowns in Eq. (12), v_1, v_2, $\ddot{p}_1(r - r_1)$ and $\ddot{p}_2(r - r_2)$; given that there are only three equations, we cannot solve for v_1 and v_2.

We therefore add one more assumption, that the target velocities v_1 and v_2 do not change over adjacent range cells r and $r + \delta$, where δ is the range sampling interval. We then obtain the simultaneous equations

$$\begin{aligned} s_{rr}(t, r) &= \ddot{p}_1(r - r_1) + \ddot{p}_2(r - r_2), \\ s_{tr}(t, r) &= v_1\ddot{p}_1(r - r_1) + v_2\ddot{p}_2(r - r_2), \\ s_{tt}(t, r) &= v_1^2\ddot{p}_1(r - r_1) + v_2^2\ddot{p}_2(r - r_2), \\ s_{rr}(t, r + \delta) &= \ddot{p}_1(r + \delta - r_1) + \ddot{p}_2(r + \delta - r_2), \\ s_{tr}(t, r + \delta) &= v_1\ddot{p}_1(r + \delta - r_1) + v_2\ddot{p}_2(r + \delta - r_2), \\ s_{tt}(t, r + \delta) &= v_1^2\ddot{p}_1(r + \delta - r_1) + v_2^2\ddot{p}_2(r + \delta - r_2). \end{aligned} \tag{14}$$

These are six equations in six unknowns, and thus, the system (14) can be solved to obtain the target velocities v_1 and v_2 as

$$v_1, v_2 = \tfrac{1}{2}(w \pm \sqrt{w^2 - 4z}), \tag{15}$$

where

$$w = \frac{s_{rr}(t, r)s_{tt}(t, r + \delta) - s_{tt}(t, r)s_{rr}(t, r + \delta)}{s_{rr}(t, r)s_{tr}(t, r + \delta) - s_{tr}(t, r)s_{rr}(t, r + \delta)}, \tag{16}$$

$$z = \frac{s_{tr}(t, r)s_{tt}(t, r + \delta) - s_{tt}(t, r)s_{tr}(t, r + \delta)}{s_{rr}(t, r)s_{tr}(t, r + \delta) - s_{tr}(t, r)s_{rr}(t, r + \delta)}. \tag{17}$$

The variables $w = v_1 + v_2$ and $z = v_1v_2$ are simply the sum and product of the velocities, respectively. In addition, we define

$$\begin{aligned} w_n &= s_{rr}(t, r)s_{tt}(t, r + \delta) - s_{tt}(t, r)s_{rr}(t, r + \delta), \\ z_n &= s_{tr}(t, r)s_{tt}(t, r + \delta) - s_{tt}(t, r)s_{tr}(t, r + \delta), \\ w_d &= s_{rr}(t, r)s_{tr}(t, r + \delta) - s_{tr}(t, r)s_{rr}(t, r + \delta). \end{aligned} \tag{18}$$

With these variables, w and z can be expressed as $w = w_n/w_d$ and $z = z_n/w_d$.

Next, w_n is rewritten as

$$\begin{aligned} w_n = &-(s_{rr}(r + \delta) - s_{rr}(r))(s_{tt}(r + \delta) + s_{tt}(r)) \\ &+ s_{rr}(r + \delta)s_{tt}(r + \delta) - s_{rr}(r)s_{tt}(r), \end{aligned} \tag{19}$$

where we omit the argument t for simplicity. Therefore, the limit of w_n/δ for $\delta \to 0$ is calculated as

$$\lim_{\delta\to 0} w_n/\delta = s_{rr}(r)s_{ttr}(r) - s_{tt}(r)s_{rrr}(r). \tag{20}$$

Similarly, we derive

$$\lim_{\delta\to 0} z_n/\delta = s_{tr}(r)s_{ttr}(r) - s_{tt}(r)s_{trr}(r), \tag{21}$$

$$\lim_{\delta\to 0} w_d/\delta = s_{rr}(r)s_{trr}(r) - s_{tr}(r)s_{rrr}(r). \tag{22}$$

As a result, the limits of w and z for $\delta \to 0$ are

$$\lim_{\delta\to 0} w = \frac{s_{rr}(r)s_{ttr}(r) - s_{tt}(r)s_{rrr}(r)}{s_{rr}(r)s_{trr}(r) - s_{tr}(r)s_{rrr}(r)}, \tag{23}$$

$$\lim_{\delta\to 0} z = \frac{s_{tr}(r)s_{ttr}(r) - s_{tt}(r)s_{trr}(r)}{s_{rr}(r)s_{trr}(r) - s_{tr}(r)s_{rrr}(r)}, \tag{24}$$

where, for example, s_{ttr} is the third order partial derivative $\partial^3 s/\partial t^2\,\partial r$.

This suggests that we can estimate the Doppler velocities v_1 and v_2 using Eq. (15) with w and z calculated as in Eqs. (23) and (24) from the second- and third-order partial derivatives of the signal $s(t, r)$. The advantage of using Eqs. (23) and (24) over Eqs. (16) and (17) is that the velocity estimates do not depend on the range sampling interval δ. In what follows, we investigate the performance of the extended texture method using Eqs. (15), (23), and (24).

The extended texture method is based on the assumption that two echoes overlap. In general, however, this assumption is not always valid. Even when there is only a single target, the method still yields two solutions v_1 and v_2, but they are less accurate than the result from the conventional texture method. To resolve this problem, we apply the extended texture method only when there are indeed two overlapping echoes, while the conventional texture method is still used when there is only a single echo. To estimate the number of targets, we use the value $\sqrt{D} = \sqrt{w^2 - 4z}$ found in Eq. (15), which is the square root of the discriminant of the quadratic formula. The proposed approach is as follows: We apply the extended texture method to the whole data set and find a discriminant whose square-root is smaller than a threshold θ_D, meaning $\sqrt{D(t, r)} < \theta_D$, to detect a region with a single echo. We apply the conventional method if this condition is satisfied and replace the estimates from the extended texture method with the velocity estimated using the conventional texture method. Consequently, the proposed method estimates the Doppler velocity (or velocities) v_{prop} by combining the conventional and extended texture methods as

$$v_{prop}(t, r) = \begin{cases} (\partial s/\partial t)/(\partial s/\partial r) & \text{if } \sqrt{D} < \theta_D, \\ (w \pm \sqrt{w^2 - 4z})/2 & \text{if } \sqrt{D} \geq \theta_D. \end{cases} \tag{25}$$

We analyze the accuracy of this proposed method in the following sections.

V. PERFORMANCE EVALUATION IN SIMULATIONS

We apply the conventional and extended texture methods and the proposed method to simulated radar data to establish their accuracy in estimating target velocities. Each target is modeled as the sum of multiple distributed points, and thus the echo $p_i(r)$ $(i = 1, 2)$ is expressed as

$$p_i(r) = \sum_{j=1}^{J} a_{i,j}q\left(r - \rho_{i,j}\right), \tag{26}$$

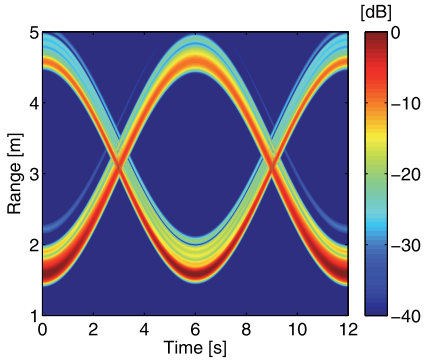

FIGURE 1. Radar signal intensity from two moving targets in the simulation.

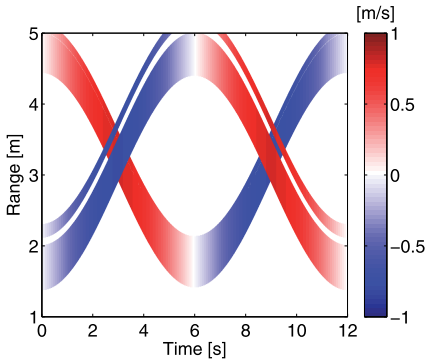

FIGURE 2. Actual Doppler velocities in the simulation.

where $q(r)$ is an echo waveform from each point target. The center frequency f_0 of $q(r)$ is 4.2 GHz, and its envelope is a raised cosine pulse with a width of 8.6 cm, corresponding to a 10-dB bandwidth of 2.2 GHz. To model echoes from a complex-shaped body such as a person, we introduce $\rho_{i,j} \geq 0$ as a positive random distance from a truncated normal distribution with a standard deviation of $\sigma = 30.0$ cm, and $a_{i,j}$ is an echo amplitude scaling factor given by $a_{i,j} = \exp(-\rho_{i,j}^2/2\sigma^2)$. We set the number of reflection points to $J = 10$ in this simulation. The model is an approximated human body with multiple reflection points distributed almost randomly, and is a simplified version of a model in [21]. The sampling frequency is 16.39 GHz, and the pulse repetition frequency is 200.0 Hz.

The received signal is generated as

$$s(t, r) = \frac{p_1(t, r - r_1(t))}{r_1(t)} + \frac{p_2(t, r - r_2(t))}{r_2(t)}, \tag{27}$$

where the propagation loss is assumed to be inversely proportional to distance because the cross section of a human-sized target is generally larger than the Fresnel zone for $f_0 = 4.2$ GHz. The target's motion is assumed to be

$$r_i(t) = R_i \cos(2\pi t/T_0) + R_0, \tag{28}$$

where $R_1 = -1.5$ m, $R_2 = 1.5$ m, $T_0 = 12.0$ s, and $R_0 = 3.0$ m. Radar signals based on these models from two moving targets were generated, and their intensities are shown in Fig. 1. The figure's ordinate and abscissa represent time t and range r. Because range $r = c\tau/2$ is determined by the time delay τ between the signal's transmission and reception, time t (horizontal axis) and delay time $\tau = 2r/c$ (vertical axis) are referred to as slow time and fast time, respectively. Figure 1 is constructed by showing the received signal intensity as a function of range r (i.e. fast time τ) when the signal is transmitted at slow time t.

We add a sequence of normally distributed complex numbers as a numerical model of additive white Gaussian noise. The signal-to-noise power ratio (S/N) depends on the signal intensity $|s(t, r)|^2$, which changes over time t and range r. The highest and lowest S/Ns are 60.0 and 27.3 dB at pulse peaks. Velocities are estimated from echoes stronger than −40.0 dB when normalized to the highest signal intensity in the following sections, so the lowest S/N is 20.0 dB in our simulation. Because we know the theoretical Doppler velocities $v_1(t) = -dr_1(t)/dt$ and $v_2(t) = -dr_2(t)/dt$, we show the velocities in Fig. 2 for t and r satisfying $|s(t, r)| > \theta_s$ with $\theta_s = 3.0 \times 10^{-3}$, where $s(t, r)$ is normalized to its maximum value. The velocity is shown only for target 1 at the 3 and 9 s intersections.

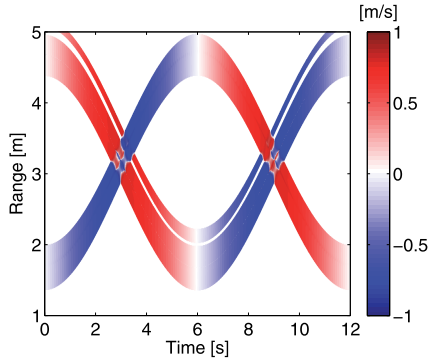

FIGURE 3. Doppler velocities $(\partial s/\partial t)/(\partial s/\partial r)$ estimated using the conventional texture method in the simulation.

By applying the conventional texture method to the simulated data, we obtain the velocity estimates in Fig. 3. We used a finite-difference approximation in calculating the time and spatial derivatives in the conventional and proposed methods. The method gives accurate estimates except at the intersection points ($t = 3$ and 9 s), where the two velocities are scrambled and incorrectly displayed. We then apply the extended texture method to the same data and obtain the Doppler velocities $v_1(t, r)$ and $v_2(t, r)$ shown in Fig. 4. Both of the Doppler velocities are correctly restored at the intersection points, but the accuracy deteriorates overall for a single target. To improve the accuracy, we need to estimate the number of targets and detect the time and range with only a single echo. As explained in the foregoing section, we estimate the number of targets using the value $\sqrt{D} = \sqrt{w^2 - 4z}$ as illustrated in Fig. 5. From this figure, it can be seen that $\sqrt{D}$ is a good indicator of the existence of multiple

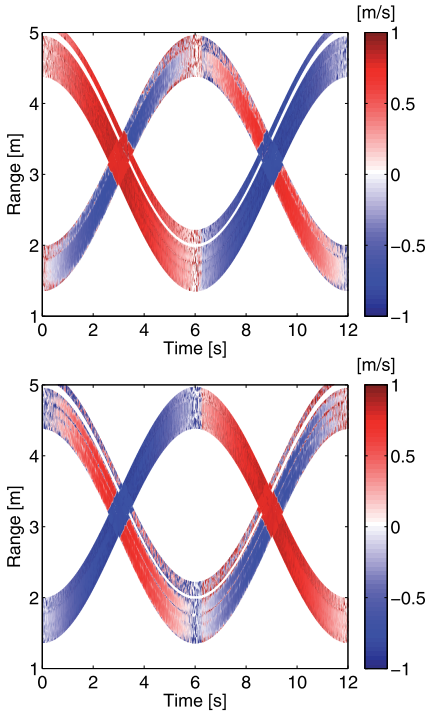

FIGURE 4. Doppler velocities $v_1(t, r)$ (top) and $v_2(t, r)$ (bottom) estimated using the extended texture method in the simulation.

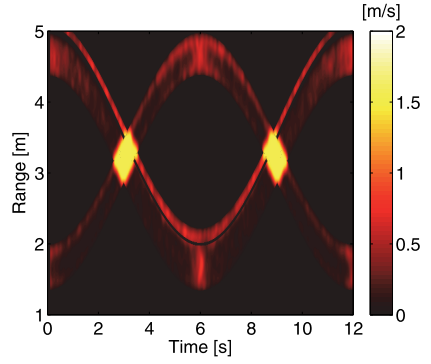

FIGURE 5. Square root of the discriminant, $\sqrt{D}$, highlighting the intersection regions at $t = 3$ and 9 s.

targets, i.e., only the two intersections at $t = 3$ and 9 s stand out.

Figure 6 shows the Doppler velocities estimated using the proposed method, which adaptively switches between the conventional and extended texture methods. We can avoid the degradation in accuracy caused by solving for two velocities when there is only a single echo. Using the proposed method, the Doppler velocities of the two targets are correctly estimated regardless of the number of targets. The estimates from the extended texture method are adopted at the $t = 3$ and 9 s intersections, while the estimate from the conventional texture method is used for the rest of the image. Consequently, the two targets are clearly separated in the two images, and their velocities are accurately estimated, compared with the actual velocities shown in Fig. 2.

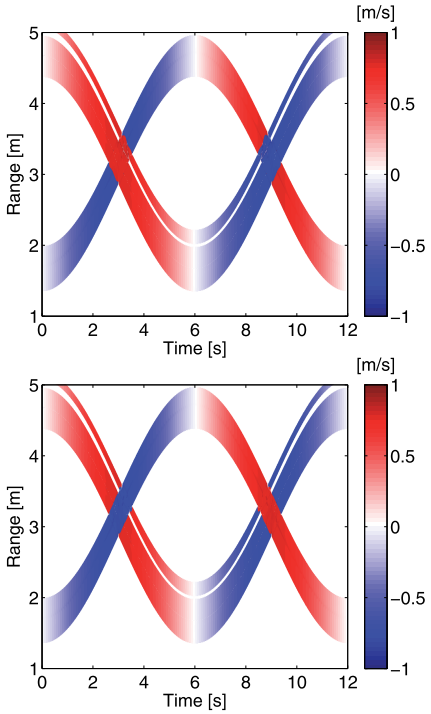

FIGURE 6. Doppler velocities $v_1(t, r)$ (top) and $v_2(t, r)$ (bottom) estimated using the proposed method combining the extended and conventional texture methods in the simulation.

For comparison, we apply the short-time Fourier transform to the simulated data and obtained the Doppler velocities shown in Fig. 7. There were 128 fast Fourier transform (FFT) points, corresponding to 0.64 s. From this figure, it can be seen that both velocities are correctly estimated but that the time resolution is compromised because of the data length in the Fourier transform. In addition, the two velocities at the points of intersection are not clearly separated.

To quantitatively compare the results, we show the Doppler velocity estimates along the actual target trajectories in Fig. 8. We note that the Doppler velocity was estimated from the largest spectral peak in the short-time Fourier transform. The accuracy of the conventional texture method is degraded when there are two echoes overlapping, whereas the extended texture method is accurate only when there are two targets at $t = 3$ and 9 s. The proposed method combines these two estimates depending on the number of targets for each time and range. The rms errors in estimated Doppler velocities was 14.0, 12.4, 0.5, and 7.4 cm/s for the conventional texture method, extended texture method, proposed method, and short-time Fourier transform, respectively. Consequently, the proposed method outperformed the conventional methods in terms of accuracy by 28 and 25 times compared with the conventional and extended texture methods, respectively. Although the accuracy of the time–frequency analysis can be improved, the main focus of this paper is not to provide accuracy comparisons with time–frequency analysis but to present an alternative approach to estimate Doppler velocities based on a completely different principle.

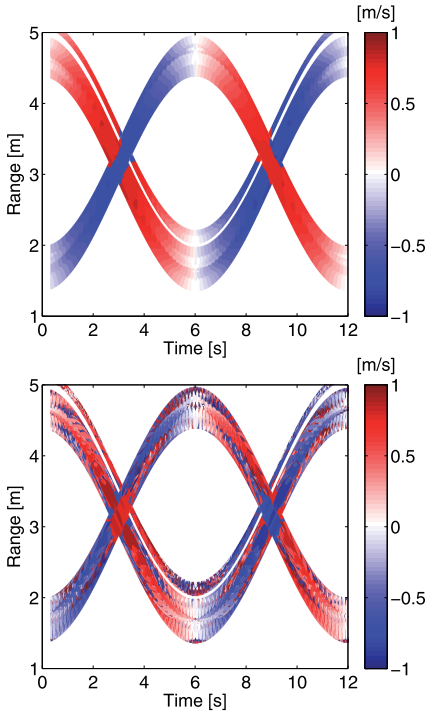

FIGURE 7. Doppler velocities estimated from the first (top) and second (bottom) largest peaks of the spectrum of the simulated data using a short-time Fourier transform in the simulation.

VI. MEASURED PERFORMANCE EVALUATION

In this section, the conventional and extended texture methods and the proposed method are applied to actual radar signals measured using an ultra-wideband radar system (PulsOn 400, Time Domain Corporation, Huntsville, AL, the USA). For this study, we use the radar data from Fig. 10 of [17]. The system is operated in the frequency band from 3.1 to 5.3 GHz with a bandwidth of 2.2 GHz corresponding to a range resolution of 6.8 cm. The transmitting and receiving antennas are dual-polarized horns (DP240, Flann Microwave Ltd., Cornwall, UK) separated by 50.0 cm.

Two targets (A and B) walk back and forth along a straight line that is the direction of the maximum gain of the antennas. Target A walks from 1.0 m away from the antennas to 5.0 m, and back to the initial point, whereas target B starts from a position 4.0 m from the antennas, walks to a position 1.0 m away, and then walks backward to 5.0 m away. The pulse-to-pulse repetition frequency is 200.0 Hz, and the Nyquist velocity is 7.14 m/s. More detailed measurement parameters can be found in [17]. Figure 9 shows a measurement setup with a person walking toward the radar antennas.

Figure 10 shows the measured radar signal intensity $|s(t, r)|^2$. The figure is constructed to show signal intensity for both slow and fast times in the same manner as Fig. 1. We see two trajectories of walking human targets. The conventional texture method is applied to the measured data and obtained the Doppler velocity estimate as shown in Fig. 11. The Doppler velocity estimated at the intersections

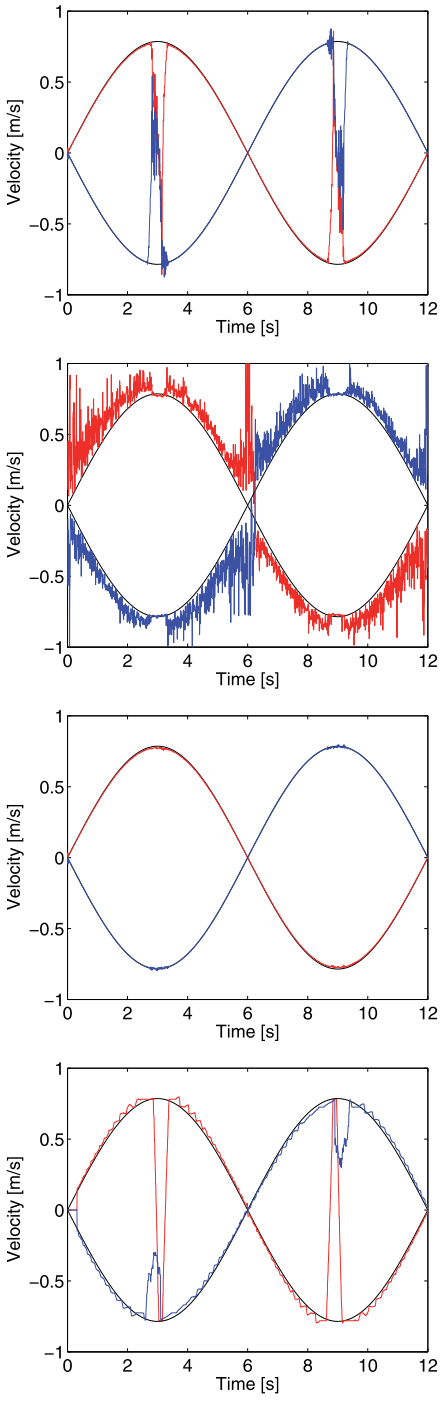

FIGURE 8. Estimated velocities (red and blue) at the actual echo ranges for the conventional texture method (top), the extended texture method (second from top), the proposed method (second from bottom), and a short-time Fourier transform (bottom), compared with the actual velocities (black) in the simulation.

shows only one of the two velocities. In contrast, by using the extended texture method, we can estimate two different Doppler velocities even at the points where two echoes overlap (see Fig. 12). The accuracy of the extended texture method, however, is degraded when there is only a single target, as was seen in the simulation results (Fig. 4).

FIGURE 9. Photograph of the experimental setup.

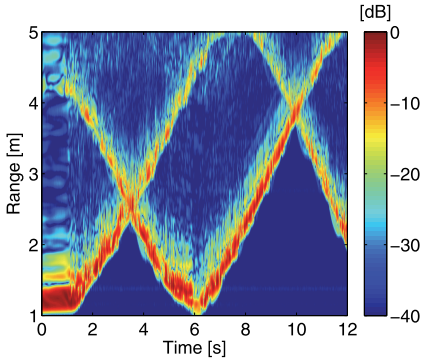

FIGURE 10. Measured radar signal intensity from two walking human targets.

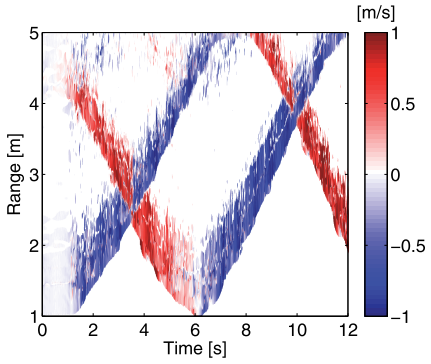

FIGURE 11. Doppler velocities $(\partial s/\partial t)/(\partial s/\partial r)$ estimated using the conventional texture method applied to measured data.

The proposed method combines the conventional and extended texture methods and estimates the Doppler velocities as shown in Fig. 13. The proposed method can estimate two target velocities even at the intersections $t = 3.5$ s and 10.0 s. For comparison, we show the Doppler velocities estimated from the first- and second-highest peaks of the spectrogram of the measurement data using the short-time Fourier transform with 128 FFT points, corresponding to 0.64 s time resolution. While the proposed method and short-time Fourier transform both can estimate two target velocities, the proposed method has the advantage of retaining high time resolution. Moreover, in the proposed method, velocities are given as closed-form solutions

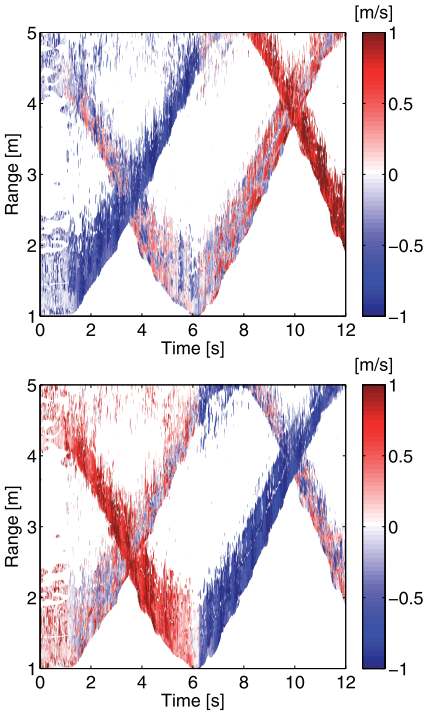

FIGURE 12. Doppler velocities $v_1(t, r)$ (top) and $v_2(t, r)$ (bottom) estimated using the extended texture method applied to measured data.

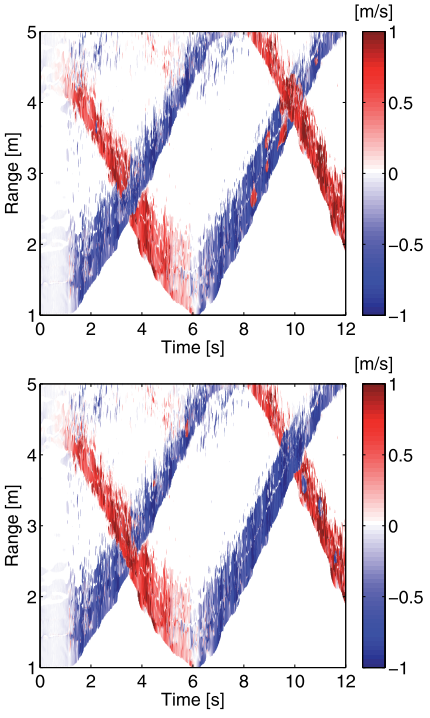

FIGURE 13. Doppler velocities $v_1(t, r)$ (top) and $v_2(t, r)$ (bottom) estimated from the measurement using the proposed method combining the extended and conventional texture methods.

of equations from local derivatives, whereas conventional time–frequency analysis techniques require searching for peaks in a spectrum. In this way, our approach, which, to the best of our knowledge, is completely novel, to estimate Doppler velocities has been demonstrated to work

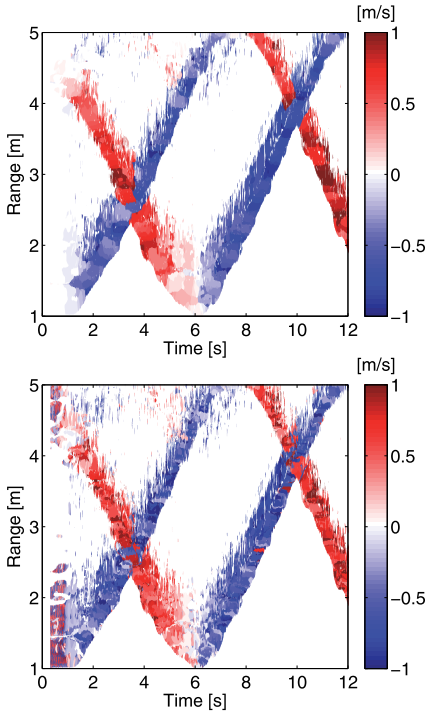

FIGURE 14. Doppler velocities estimated from the first (top) and second (bottom) largest peaks of spectrum of measurement data using short-time Fourier transform.

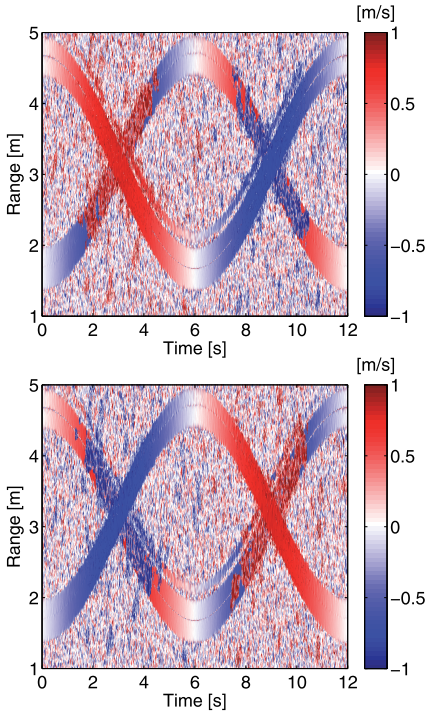

FIGURE 15. Doppler velocities $v_1(t, r)$ (top) and $v_2(t, r)$ (bottom) estimated using the proposed method in a simulation with the highest S/N of 20.0 dB (and the lowest S/N of −12.7 dB).

with both simulated and measured data, and it moreover does not require generating Doppler spectra, which distinguishes the method from the various time–frequency analysis techniques.

VII. DISCUSSION

A. DEFINITION OF TARGET

In this paper, the word 'target' has been used without definition, but which is addressed here. In simulations and measurements (Sections V and VI), we assumed two human targets, where 'target' means a set of scattering centers that lie in the vicinity and have almost the same velocity. For example, the numerical target model introduced in Section V consists of multiple scattering centers moving at the same speed, where the body parts were assumed to have the same velocity. Nevertheless, various parts of an actual walking human have different velocities; considering a human as a single-velocity target is only an approximation. The proposed method is also applicable when multiple body parts move at different speeds, implying that the scope of the proposed method includes micro-Doppler analysis, which is known to be useful in target classification as stated in Section I.

B. EXTENSION OF THE PROPOSED METHOD

Here, we discuss whether the proposed method can be extended to more than two targets. Let us assume three moving targets overlapping in the range-time domain. The received signal can be expressed as

$$s(t, r) = p_1(t, r - r_1(t)) + p_2(t, r - r_2(t)) + p_3(t, r - r_3(t)).$$

Third-order partial derivatives of $s(t, r)$ are

$$\begin{aligned}
s_{rrr}(t, r) &= \dddot{p}_1(r - r_1) + \dddot{p}_2(r - r_2) + \dddot{p}_3(r - r_3),\\
s_{trr}(t, r) &= v_1\ddot{p}_1(r - r_1) + v_2\ddot{p}_2(r - r_2) + v_3\ddot{p}_3(r - r_3),\\
s_{ttr}(t, r) &= v_1^2\dot{p}_1(r - r_1) + v_2^2\dot{p}_2(r - r_2) + v_3^2\dot{p}_3(r - r_3),\\
s_{ttt}(t, r) &= v_1^3\dddot{p}_1(r - r_1) + v_2^3\dddot{p}_2(r - r_2) + v_3^3\dddot{p}_3(r - r_3),
\end{aligned}$$

where there are four equations with six unknowns, and thus these simultaneous equations cannot be solved uniquely. We need to introduce then a similar approximation as used in Section IV; the velocities v_1, v_2, and v_3 are unchanged over three neighboring range bins r, $r + \delta$, and $r + 2\delta$. As a result, we obtain $3 \times 4 = 12$ equations with 12 unknowns, which can be solved using the closed-form solution for a cubic equation, which means the proposed method can be extended to instances with three targets.

In a similar way, it is expected that the proposed method can be extended to instance with more than three targets; the computational load depends mostly on the calculation of the solution of polynomial equations. We also note that, according to Galois theory, there are no closed-form solutions for more polynomials of order five, and therefore it is necessary to employ a numerical solver instead of relying on closed-form solutions, which would increase the computational load.

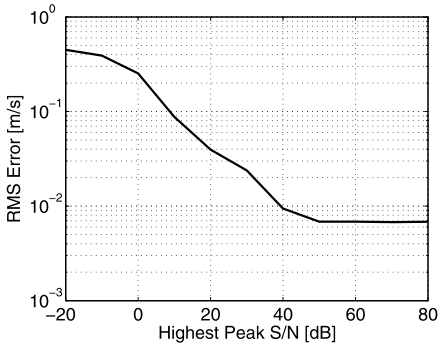

FIGURE 16. Root-mean-square error in estimating velocities using the proposed method with various highest S/N.

C. NOISE TOLERANCE OF THE PROPOSED METHOD

In comparing Figs. 6 and 13, the simulation results (Fig. 6) show a smoother velocity distribution than the measured results (Fig. 13). This is partly because of the simplified numerical target model in our simulation, although other undesirable effects in the measurement (e.g. noise, interference and multi-path) could be the reason. We assumed a relatively high S/N (the highest and lowest S/N of 60.0 dB and 27.3 dB) in the simulations in Section V. To clarify the effect of noise on the accuracy of the proposed method, we conducted additional simulations using various S/N values. For example, we assume the highest and lowest S/N to be 20.0 dB and -12.7 dB in the simulation, and obtain Doppler velocities estimated using the proposed method (see Fig. 15), which exhibit rougher velocity distributions.

To evaluate the accuracy in a noisy situation quantitatively, Fig. 16 shows the root-mean-square (RMS) error in estimating velocities using the proposed method for various highest S/N. We note that the lowest S/N is always 32.7 dB lower than this value in our simulation. This figure indicates that to achieve an RMS error of 1.0 cm/s, the highest and lowest S/N must be higher than 38.0 dB and 5.3 dB, respectively. Although the degradation in accuracy because of other factors such as interference and multi-path effects could be inferred from this result, more detailed studies are necessary to address these more practical issues.

VIII. CONCLUSION

We have proposed a method for estimating Doppler velocities without forming spectra by using the solutions of simultaneous equations from the local derivatives of ultra-wideband radar signals. We first derived an extended version of the conventional texture method that allows two Doppler velocities to be directly estimated from overlapping echoes. Then we proposed a method combining the conventional and extended texture methods depending on the number of targets in each range. Unlike conventional time-frequency analysis, the proposed method is free from the trade-off between time and frequency resolution, resulting in a high time resolution. The conventional and proposed methods were both applied to simulated and measured data, and it was confirmed that the proposed method can obtain accurate velocity estimates without finding the peaks of spectra. Based on this study, an important task, left as an open problem, is to compare quantitatively the accuracy and resolution of the proposed and conventional methods using measured data.

REFERENCES

[1] A. B. del Campo, F. Le Chevalier, and A. Yarovoy, "Exploiting range migration for unambiguous velocity measurements," in *Proc. 16th Int. Radar Symp.*, 2015, pp. 309–314.
[2] E. J. Barlow, "Doppler radar," in *Proc. IRE*, vol. 37. no. 4, pp. 340–355, Apr. 1949.
[3] J. R. Klauder, "The design of radar signals having both high range resolution and high velocity resolution," *Bell Syst. Tech. J.*, vol. 39, no. 4, pp. 809–820, Jul. 1960.
[4] T. Claasen and W. Mecklenbrauker, "The aliasing problem in discrete-time Wigner distributions," *IEEE Trans. Acoust., Speech, Signal Process.*, vol. 31, no. 5, pp. 1067–1072, Oct. 1983.
[5] D. T. Barry, "Fast calculation of the Choi–Williams time-frequency distribution," *IEEE Trans. Signal Process.*, vol. 40, no. 2, pp. 450–455, Feb. 1992.
[6] S. S. Ram and H. Ling, "Application of the reassigned joint time-frequency transform to wideband scattering from waveguide cavities," *IEEE Antennas Wireless Propag. Lett.*, vol. 6, pp. 580–583, 2007.
[7] F. Gran, A. Jakobsson, and J. A. Jensen, "Adaptive spectral Doppler estimation," *IEEE Trans. Ultrason., Ferroelect., Freq. Control*, vol. 56, no. 4, pp. 700–714, Apr. 2009.
[8] L. Du, J. Li, P. Stoica, H. Ling, and S. S. Ram, "Doppler spectrogram analysis of human gait via iterative adaptive approach," *Electron. Lett.*, vol. 45, no. 3, pp. 186–188, Jan. 2009.
[9] V. C. Chen, "Doppler signatures of radar backscattering from objects with micro-motions," *IET Signal Process.*, vol. 2, no. 3, pp. 291–300, Sep. 2008.
[10] R. G. Raj, V. C. Chen, and R. Lipps, "Analysis of radar human gait signatures," *IET Signal Process.*, vol. 4, no. 3, pp. 234–244, 2010.
[11] M. Gustafsson, A. Andersson, T. Johansson, S. Nilsson, A. Sume, and A. Orbom, "Extraction of human micro-Doppler signature in an urban environment using a 'sensing-behind-the-corner' radar," *IEEE Geosci. Remote Sens. Lett.*, vol. 13, no. 2, pp. 187–191, Feb. 2016.
[12] A. Lin and H. Ling, "Frontal imaging of human using three-element Doppler and direction-of-arrival radar," *Electron. Lett.*, vol. 42, no. 11, pp. 660–661, May 2006.
[13] A. Lin and H. Ling, "Doppler and direction-of-arrival (DDOA) radar for multiple-mover sensing," *IEEE Trans. Aerosp. Electron. Syst.*, vol. 43, no. 4, pp. 1496–1509, Oct. 2007.
[14] K. Saho, T. Sakamoto, T. Sato, K. Inoue, and T. Fukuda, "Pedestrian imaging using UWB Doppler radar interferometry," *IEICE Trans. Commun.*, vol. E96-B, no. 2, pp. 613–623, 2013.
[15] Y. Kim and H. Ling, "Human activity classification based on micro-Doppler signatures using a support vector machine," *IEEE Trans. Geosci. Remote Sens.*, vol. 47, no. 5, pp. 1328–1337, May 2009.
[16] Y. He, P. Molchanov, T. Sakamoto, P. Aubry, F. Le Chavalier, and A. Yarovoy, "Range-Doppler surface: A tool to analyze human target in ultra-wideband radar," *IET Radar, Sonar Navigat.*, vol. 9, no. 9, pp. 1240–1250, 2015.
[17] T. Sakamoto, T. Sato, P. J. Aubry, and A. G. Yarovoy, "Texture-based automatic separation of echoes from distributed moving targets in UWB radar signals," *IEEE Trans. Geosci. Remote Sens.*, vol. 53, no. 1, pp. 352–361, Jan. 2015.
[18] Y. Kim, S. Choudhury, and H.-J. Kong, "Application of micro-Doppler signatures for estimation of total energy expenditure in humans for walking/running activities," *IEEE Access*, vol. 4, pp. 1560–1569, 2016.
[19] L. Du, L. Li, B. Wang, and J. Xiao, "Micro-Doppler feature extraction based on time-frequency spectrogram for ground moving targets classification with low-resolution radar," *IEEE Sensors J.*, vol. 16, no. 10, pp. 3756–3763, May 2016.
[20] D. P. Fairchild and R. M. Narayanan, "Multistatic micro-Doppler radar for determining target orientation and activity classification," *IEEE Trans. Aerosp. Electron. Syst.*, vol. 52, no. 1, pp. 512–521, Feb. 2016.
[21] S. Chang, R. Sharan, M. Wolf, N. Mitsumoto, and J. W. Burdick, "UWB radar-based human target tracking," in *Proc. IEEE Radar Conf.*, May 2009, pp. 1–6, doi: 10.1109/RADAR.2009.4977001.

TAKUYA SAKAMOTO (M'04) received the B.E. degree in electrical and electronic engineering from Kyoto University, Kyoto, Japan, in 2000, and the M.E. and Ph.D. degrees in communications and computer engineering from the Graduate School of Informatics, Kyoto University, in 2002 and 2005, respectively. From 2006 to 2015, he was an Assistant Professor with the Graduate School of Informatics, Kyoto University. From 2011 to 2013, he was also a Visiting Researcher with the Delft University of Technology, Delft, The Netherlands. Since 2015, he has been an Associate Professor with the Graduate School of Engineering, University of Hyogo, Himeji, Japan. He has also been a Project Researcher with the Graduate School of Informatics, Kyoto University, since 2015. His current research interests lie in ultra-wideband radar, radar imaging, and radar signal processing. He received the Best Paper Award from the International Symposium on Antennas and Propagation in 2004, the Young Researcher's Award from the IEICE in 2007, the Best Presentation Award from the IEEJ in 2007, the Best Paper Award from the IEICE Communication Society in 2007, the Best Paper Award from ISAP2012 in 2012, and the Masao Horiba Award in 2016.

DAICHI AKIYAMA received the B.E. degree in electrical and electronic engineering from Kyoto University, Kyoto, Japan, in 2014, where he is currently pursuing the M.E. degree in communications and computer engineering with the Graduate School of Informatics.

TAKURO SATO is currently pursuing the B.E. degree in electrical and electronic engineering with Kyoto University, Kyoto, Japan.

TORU SATO (M'92) received the B.E., M.E., and Ph.D. degrees in electrical engineering from Kyoto University, Kyoto, Japan in 1976, 1978, and 1982, respectively. He has been with Kyoto University, since 1983, where he is currently a Professor with the Department of Communications and Computer Engineering, Graduate School of Informatics. His major research interests have include system design and signal processing aspects of UWB radars, atmospheric radars, radar remote sensing of the atmosphere, and biomedical imaging. He is a fellow of the Institute of Electronics, Information, and Communication Engineers of Japan, and a member of the Society of Geomagnetism and Earth, Planetary and Space Sciences, the Japan Society for Aeronautical and Space Sciences, the Institute of Electrical and Electronics Engineers, and American Meteorological Society.